A Crosstalk Study on Metamaterial-Inspired Substrate Integrated Waveguides

Michalis Nitas*, Vasileios Salonikios*, Traianos Yioultsis*, Theodoros Zygiridis†, Nikolaos Kantartzis* and Stamatios Amanatiadis*

*Aristotle University of Thessaloniki, Department of Electrical and Computer Engineering, Thessaloniki, Greece

†University of Western Macedonia, Department of Electrical and Computer Engineering, Kozani, Greece

mnitas@auth.gr

***Abstract*—Substrate Integrated Waveguide (SIW) is a well-established technology in the mm-wave frequency range with several related applications of mm-wave components and antennas. Recently, the Broadside-Coupled Complementary Split-Ring Resonator SIW (BC-CSRR SIW) has been proposed as an alternative to the classical SIW design, utilizing printed resonant metamaterials instead of metallic vias. In this work we explore the wave confinement capability of the BC-CSRR SIW through numerical crosstalk studies. A parametric study is carried out for the minimization of leakage losses, followed by a numerical calculation of crosstalk between adjacent waveguides. BC-CSRR SIW results are compared with the classical SIW configuration exhibiting equivalent behavior.**

***Index Terms*—crosstalk, electromagnetic field confinement, metamaterial-inspired SIWs, substrate integrated waveguides.**

I. Introduction

Utilization of higher frequency zones in mm-wave communications with the subsequent design of mm-wave components is one of the effects of the emerge of 5G communications. One of the most characteristic examples of low-cost, easy-to-fabricate planar structures is the technology of the Substrate Integrated Waveguide (SIW) [1]–[5]. Recently, an alternative metamaterial-inspired SIW was proposed, exhibiting equivalent characteristics, the Broadside-Coupled Complementary Split-Ring Resonator SIW (BC-CSRR SIW) [6], with its most prominent advantage versus the classical version of the SIW being its fully-planar property due to the avoidance of via hole drilling. Additionally, utilization of this waveguiding structure has already led to the design of many leaky-wave antennas and other mm-wave components [7]–[9], whereas an advanced modification of the initial BC-CSRR SIW has already been proposed, with the incorporation of edge-coupled SRRs (EC-CSRR SIW) [10].

Electromagnetic field confinement in SIWs at their vertical dimension is guaranteed due to their termination on the conductors' surface, whereas there is a certain amount of leakage at their lateral direction, which depends on the dimensions and spacing of the utilized particles (metallic vias or split-ring resonators) and consequently results in leakage losses [11]–[14]. This paper focuses on the numerical calculation of the forward crosstalk in adjacent BC-CSRR SIWs and compares its performance with the corresponding classical SIW structure at X-band. Fabrication and measurement of the simulated structures, for the production of experimental results and comparison with the simulated ones is under study and will be presented in an upcoming publication.

II. Wave Propagation in SIW Structures

A. Comparison Between BC-CSRR SIW and Classical SIW

Initially, we assess the waveguiding capability of the BC-CSRR SIW at X-band. A very detailed design and optimization process of this waveguide is presented in [6]: Equivalent circuit theory is utilised for the choice of the optimal dimensions of the BC-CSRR meta-particles, a full-wave numerical eigenvalue study of the waveguide's unit cell is performed, based on the robust **E-B** Bloch Floquet FEM formulation [15], [16], combined with wave propagation (excitation) simulations and experimental results. Here, we utilize the optimized dimensions obtained for X-band operation, which are summarized in Table I and visualized in Fig. 1, which illustrates the BC-CSRR SIW unit cell. The classical SIW dimensions, optimized for operation at X-band, are $d_{\rm SIW} = 1$ mm and $p_{\rm SIW} = 2$ mm, (via diameter and via spacing, respectively) [1]–[4]. Both configurations are designed on a substrate of thickness $h = 1.5113$ mm, dielectric constant $\epsilon_{\rm r} = 2.95$ and loss tangent $\tan\delta = 0.0018$. A proper matching circuit is designed, depicted in Fig. 2, optimized for operation at $8 - 12$ GHz, consisting of a tapered microstrip line, with dimensions $w_{\rm m} = 3.87$ mm (exhibiting a characteristic impedance $Z_0 = 50$ Ohm), $l_{\rm m} = 23.22$ mm, $w_{\rm tap} = 7$ mm and $l_{\rm tap} = 5.236$ mm [6], [10]. Feeding of the simulated waveguides is done with SMA connectors. Both structures have a total length of $L_{\rm tot} = 107$ mm. It is noted that all simulations are carried out in Comsol Multiphysics™.

In Fig. 3, the simulated S-parameters are illustrated. It is easily observed that the BC-CSRR SIW possesses a very good waveguiding capability, with a transmission loss of less than -2 dB inside the simulated frequency zone, and a very

TABLE I
Optimal Dimensions of the Proposed BC-CSRR SIW

Central frequency (GHz)	Ring radius r (mm)	Ring width d (mm)	Ring gap g (mm)	SIW width w (mm)	Substrate height h (mm)
10	2.2	1.4	0.8	13.5	1.5113

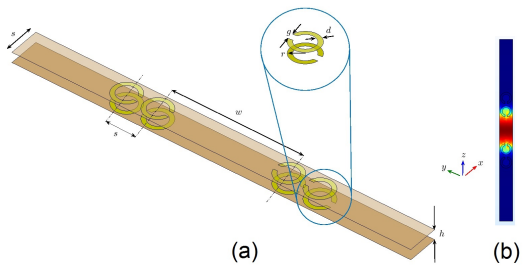

Fig. 1. (a) Geometric parameters of the BC-CSRR SIW unit cell: effective width between the center of the rings (w), ring period (s), ring gap (g), ring external radius (r), ring width (d) and pcb width (h). The propagation axis is the x axis (b) Distribution of electric field norm (V/m) at 10 GHz at mid-substrate plane (taken from an eigenvalue study [6]).

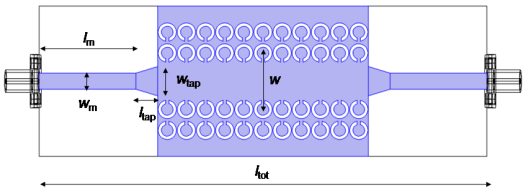

Fig. 2. Matching circuit and SMA feeding for the BC-CSRR SIW. Microstrip dimensions designed for a 50 Ohm impedance, whereas the tapering dimensions result from an optimization procedure.

low average return loss, exhibiting an equivalent behavior versus the classical SIW. It is noted that transmission loss consists of all types of losses, i.e. dielectric loss, conductor loss and (lateral) leakage loss. Additionally, the dominant field component E_z at 9 GHz at the middle of the substrate for the BC-CSRR SIW and the SIW is illustrated in Fig. 4(a) and 4(b), respectively.

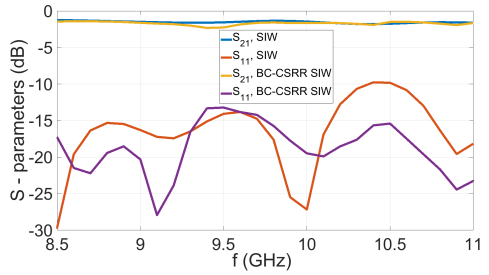

Fig. 3. Simulated S-parameters of the BC-CSRR SIW and the classical SIW. Both waveguides exhibit equivalent results, with transmission loss less than -2 dB inside the simulated frequency zone.

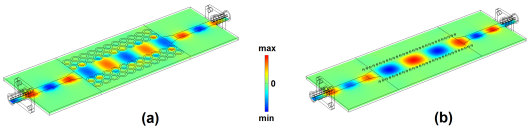

Fig. 4. Field distribution of the dominant electric component (E_z) at 9 GHz at mid-substrate plane for the BC-CSRR SIW (a) and the classical SIW (b).

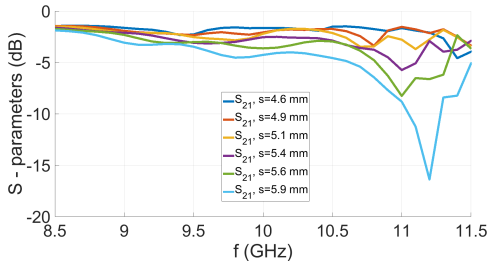

Fig. 5. Simulated S_{21}-parameter of a BC-CSRR SIW for varying spacing period values s. Transmission loss increases with the increase of spacing.

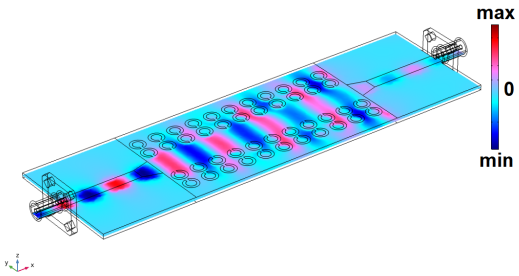

Fig. 6. Dominant electric field component E_z at mid-substrate plane at 9 GHz of a BC-CSRR SIW waveguide with a period $s = 5.9$ mm. There is an observable lateral leakage causing restricted waveguiding capability.

B. Leakage Loss Minimization of the BC-CSRR SIW for X-band Operation

Here, we present a parametric analysis of the period s of the unit cell of the waveguide, in order to minimize the lateral leakage losses. Therefore, according to Fig. 1, we vary the parameter s, in order to observe the leakage loss behavior of the waveguide. Fig. 5 illustrates the S_{21} parameters versus frequency for different spacing values. It is easily observed that transmission loss increases with the increase of s, whereas the optimal value which minimizes the leakage losses is $s = 4.6$ mm. It is noted that smaller s values return equal results, but increase the number of degrees of freedom due to the proximity of the resonators (the lower distance limit where two adjacent resonators are in contact is 4.4 mm). Fig. 6 visualises the aforementioned statement: Illustration of the normal electric field component (dominant) E_z at 9 GHz at the middle of the substrate for the maximum simulated spacing $s = 5.9$ mm, proves that the electromagnetic wave leaks outside the waveguide and cannot be confined inside the waveguiding channel. Therefore, in this case, the waveguide's capability of guiding the electromagnetic wave is restricted.

III. Numerical Calculation of Crosstalk

In this section, we assess the electromagnetic field confinement capability of the simulated waveguides. This is done by numerically calculating the forward crosstalk between two adjacent waveguiding structures: The BC-CSRR SIW structure consists of two adjacent BC-CSRR SIWs, which share two

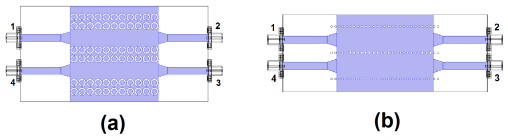

Fig. 7. Crosstalk calculation structures for the BC-CSRR SIW (a) and the classical SIW (b). Both structures are excited on port 1 via coaxial SMA connectors. Crosstalk evaluation refers to the S_{31} parameter value.

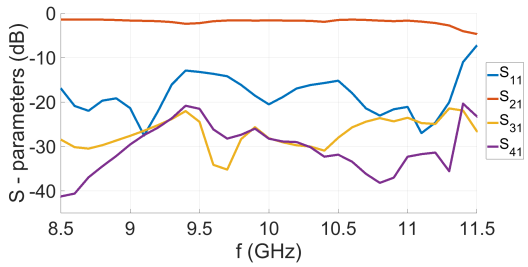

Fig. 8. Simulated S-parameters of the crosstalk structure of the BC-CSRR SIW. S_{31} remains below -22 dB within the simulated frequency zone.

common rows of CSRRs, whereas in the classical SIW case, two adjacent SIW waveguides share a common row of vias. SMA connectors are also utilized to feed the structures at port 1, whereas the receiving signal is calculated at ports 2, 3 and 4 (Fig. 7). In Fig. 8 the calculated S-parameters for the BC-CSRR SIW case are illustrated. It is easily observed that the crosstalk value S_{31} remains below -22 dB within the simulated frequency zone. Additionally, the returned S-parameters for the classical SIW case are depicted in Fig. 9, where equivalent results are returned, as well. Therefore, the fine wave confinement capability of the BC-CSRR SIW is confirmed, along with its equivalence with the classical SIW. Finally, the dominant field components E_z for the BC-CSRR SIW and the classical SIW cases at 9 GHz are illustrated in Figs. 10 and 11, respectively, at the mid-planes of the dielectric substrates, exhibiting both structures' absolute capability of electromagnetic field confinement.

IV. Conclusion

We have presented a numerical study on the calculation of crosstalk in BC-CSRR SIWs. Initially, the waveguiding capability of the metamaterial-based SIW is explored, through the parametric study of varying distance between the resonators. The optimal configuration of the waveguide is subsequently placed in a structure, where two adjacent waveguides share two common rows of CSRRs, forming a 4-port network excited in one port. Numerical results exhibit equivalent behavior compared with the classical SIW ones.

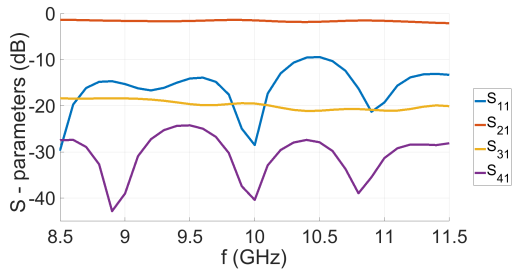

Fig. 9. Simulated S-parameters of the crosstalk structure of the classical SIW. S_{31} remains below -20 dB within the simulated frequency zone.

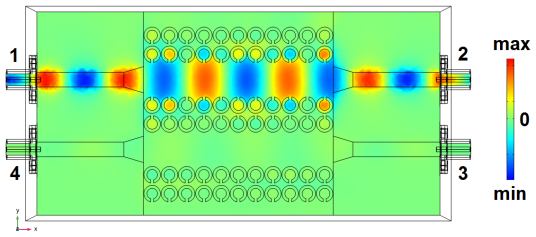

Fig. 10. E_z component at 9 GHz at mid-substrate of the BC-CSRR SIW crosstalk structure.

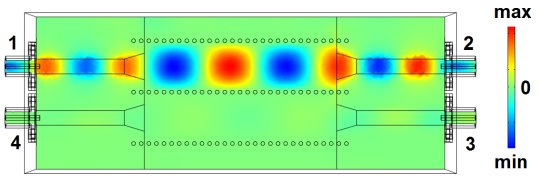

Fig. 11. E_z component at 9 GHz at mid-substrate of the classical SIW crosstalk structure.

Acknowledgment

The research project was supported by the Hellenic Foundation for Research and Innovation (H.F.R.I.) under the "2nd Call for H.F.R.I. Research Projects to support Post-Doctoral Researchers" (Project Number: 756).

References

[1] M. Bozzi, A. Georgiadis, K. Wu, "Review of substrate-integrated waveguide circuits and antennas," *IET Microw. Antennas Propag.*, vol. 5, no. 8, pp. 909–920, 2011.

[2] D. Deslandes, K. Wu, "Accurate modeling, wave mechanisms, and design considerations of a substrate integrated waveguide," *IEEE Trans. Microw. Theory Tech.*, vol. 54, no. 6, pp. 2516–2526, 2006.

[3] F. Xu and K. Wu, "Guided-wave and leakage characteristics of substrate integrated waveguide," *IEEE Trans. Microw. Theory Tech.*, vol. 53, no. 1, pp. 66-72, 2005.

[4] D. Deslandes, K. Wu, "Single-substrate integration technique of planar circuits and waveguide filters," *IEEE Trans. Microw. Theory Tech.*, vol. 51, no. 2, pp. 593–596, 2003.

[5] J. Liu, D. R. Jackson, Y. Long, "Substrate integrated waveguide (SIW) leaky-wave antenna with transverse slots," *IEEE Trans. Antennas Propag.*, vol. 60, no. 1, pp. 20-29, 2012.

[6] M. Nitas, M. T. Passia, and T. V. Yioultsis, "Fully Planar Slow-wave Substrate Integrated Waveguide based on Broadside-coupled Complementary Split Ring Resonators for mmWave and 5G Components," *IET Microw. Antennas Propag.*, vol. 14, no. 10, pp. 1096-1107, Jun. 2020.

[7] M. Nitas, S. Raptis, V. Salonikios and T. V. Yioultsis, "Fully planar CSRR-SIW slot antennas of optimized gain and enhanced bandwidth for millimeter wave and 5G communications," *2019 International Workshop on Antenna Technology (iWAT), IEEE*, pp. 47-79, Mar. 2019.

[8] V. Salonikios, M. Nitas, S. Raptis, and T. V. Yioultsis, "Design of a Fully Planar BC-CSRR SIW-based H-plane Sectoral Horn with a Printed Transition," *2019 13th European Conference on Antennas and Propagation (EuCAP), IEEE*, pp. 1-5, Mar. 2019.

[9] O. Christogeorgos, M. T. Passia, M. Nitas, and T. V. Yioultsis, "Design of fully-planar CSRR-based substrate integrated waveguide circuits," *2019 International Conference on Electromagnetics in Advanced Applications (ICEAA), IEEE*, pp. 0289-0293, Sep. 2019.

[10] M. T. Passia, and T. V. Yioultsis, "A Uniplanar Substrate Integrated Waveguide based on Edge-coupled Complementary Split-ring Resonators for Millimeter-wave Components," *15th European Conference on Antennas and Propagation (EuCAP), IEEE*, pp. 1-5, Mar. 2021.

[11] M. Pasian, M. Bozzi and L. Perregrini, "Crosstalk in substrate integrated waveguides," *IEEE Trans. Electromagn. Compat.*, vol. 57, no. 1, pp. 80-86, Dec. 2014.

[12] M. Pasian, M. Bozzi and L. Perregrini, "A formula for radiation loss in substrate integrated waveguide," *IEEE Trans. Microw. Theory Tech.*, vol. 62, no. 10, pp. 2205-2213, Oct. 2014.

[13] M. Pasian, M. Bozzi and L. Perregrini, "Radiation losses in substrate integrated waveguides: A semi-analytical approach for a quantitative determination," *IEEE MTT-S International Microwave Symposium Digest (MTT)*, pp. 1-3, Jun. 2013.

[14] A. Scogna and A. Orlandi, "Systematic analysis of the signal integrity performance of surface integrated waveguide structures (SIWs)," *IEEE International Symposium on Electromagnetic Compatibility*, pp. 784-789, Jul. 2010.

[15] M. Nitas, C. S. Antonopoulos, and T. V. Yioultsis, "E-B eigenmode formulation for the analysis of lossy and evanescent modes in periodic structures and metamaterials," *IEEE Trans. Magn.*, vol. 53, no. 6, pp. 1-4, Jun. 2017.

[16] M. Nitas *et al.,* "Numerical Calculation of Dispersion Diagrams and Field Distributions of Waves in 3-D Periodic Split-Ring Resonator Media," *IEEE Trans. Magn.*, vol. 55, no. 12, pp. 1-4, Dec. 2019.